Detection of drainage channel networks on digital satellite images

C. ICHOKU, A. KARNIELI

Jacob Blaustein Institute for Desert Research, Ben-Gurion University of the Negev, Sede-Boker Campus 84990, Israel

A. MEISELS

Department of Mathematics and Computer Science, Ben-Gurion University of the Negev, Beer-Sheva 84105, Israel

and J. CHOROWICZ

Laboratoire de Géologie-Géomorphologie Structurale et Télédétection, Université Pierre et Marie Curie, Tour 26, 4 Place Jussieu, 75252 Paris, France

Abstract. We present a technique for automatic detection of drainage channel networks on single digital images acquired by conventional remote sensing satellites such as Landsat and SPOT. Since these satellites are Sun-synchronous, the approximate local Sun angle at time of image acquisition is always known. Consequently, the spatial behaviour of shading with respect to channels and other topo-morphological features is known. This knowledge has been used to advantage in this work.

We use a multi-level knowledge-based approach for this detection process. The first and lowest level deals with image processing: radiometric and edge enhancement, edge detection and consolidation, and skeletonization; resulting in a complex network of lines. The second (intermediate) level of knowledge for network extraction performs a categorization of line segments in order of resemblance to channel elements based on the strength and local disposition of shading. The highest level of knowledge that has been applied, reconstructs the channel network from the selection of these line segments based on structural considerations, including connectivity and streamflow direction. This last stage of network extraction conforms naturally to a global view of a network. The extracted networks are smooth and relatively well connected and seem to be quite encouraging for developing this approach further into practical uses.

1. Introduction

The extraction and analysis of drainage networks is an effective way of studying Earth-based features and phenomena. Indeed, drainage networks constitute one of the most widely applicable features in the geosciences. For instance, they often form the basis upon which the morphology and pattern of landscapes are characterized, and many geological conclusions are based on inferences derived from them. Furthermore, almost all maps contain drainage channel networks, to a greater or lesser extent, for reference.

Manual methods have been traditionally used to extract drainage networks from either field data, topographical maps, aerial photographs, satellite images, or any combination of these. Over the past decade, much work has been done on automating the extraction of drainage networks, although almost all algorithms use Digital

Elevation Models (DEMs) as base data (e.g., Chorowicz *et al.* 1992). This is evidently due to the fact that DEMs express terrain morphology directly in a discrete fashion, and, as such, are conveniently disposed for flow modelling and drainage network extraction.

However, DEMs are not readily available at reasonable costs for most areas of the world requiring drainage network based studies, unlike satellite images which can be acquired for most parts of the Earth's surface on a routine basis. So far, mainly manual procedures have been employed in extracting drainage networks from satellite images (Astaras 1985, Astaras *et al.* 1990). In an attempt to develop a computerized approach, Benhamou (1987) used an inference method based on the differences between the spectral properties of bare soil and vegetation to extract drainage features characterized by the concentration of vegetation within valleys in an otherwise arid region from Landsat MSS images.

Apart from spectral information, satellite images indirectly express surface morphology through topographic shading which occurs especially in certain wave bands. This shading property was utilised by Wang *et al.* (1983) to develop an approach for extracting ridge and valley lines from single satellite images. They applied their technique to Landsat MSS band 7 data. Although they offered several suggestions for the use of high level spatial reasoning in detection procedures, especially as applied to valleys (or channels), these were not implemented in their work. Their approach was limited to the use of what may be considered as low and intermediate levels of reasoning. They performed grey-level thresholding followed by region boundary detection to generate lines (low level), and subsequently, each unbranched segment of these lines was classified as either a ridge or a valley segment based on its local characteristics alone (intermediate level).

In this paper, we present an advanced computerized methodology for extracting drainage channel networks (or simply, channel networks) from single digital satellite images. Our methodology uses a series of techniques at different (low, intermediate, and high) levels of abstraction of image understanding (Meisels 1991). The proposed approach applies to images acquired by remote sensing satellites operating in the visible/infrared regions of the electromagnetic spectrum such as Landsat and SPOT. We do not consider other types of satellite images such as thermal or radar images.

2. Theoretical considerations

Visible/infrared sensors of the type addressed in this work (such as Landsat and SPOT) are flown in Sun-synchronous satellites. As such, image acquisition is done at approximately the same local Sun time regardless of place. This is usually in the mid-morning hours, about 9:30 a.m. for Landsat (cf. Freden and Gordon 1983, p. 537). At this time of day, the Sun is always located in the general east direction. Although there may be variations in Sun azimuth and zenith angle from place to place, for an area covered in a single scene, this variation is negligible and direction of sunlight may be considered constant. The brightness expressed by an elementary surface (pixel) in a visible/infrared image is a function of both the illumination it receives and its reflectance. Topographical reflectance depends on several factors including lithology, vegetation, land use, as well as soil moisture, mineral, and organic matter content. Detailed discussion of the influence of these factors can be found in most standard remote sensing books, and will not be undertaken here. However, assuming uniform reflectance characteristics—which is obtainable for a limited area—image brightness will depend on illumination which is related to surface
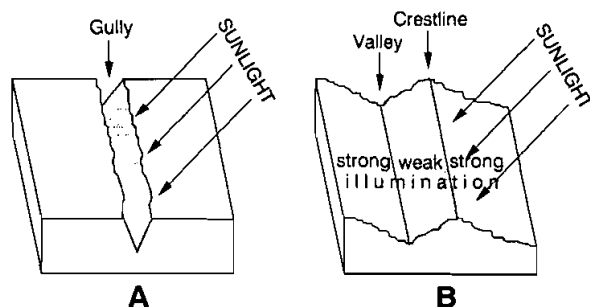
Figure 1. Illustration of topographical illumination and shading in relation to the direction of sunlight for (a) Gully, (b) Valley and Crestline.

exposure and orientation with respect to the direction of sunlight. This relation is of great importance in the recognition of drainage channels in images.

The effect of illumination of drainage channels on the image can be demonstrated for two categories of channels, namely, gullies with steep walls and valleys formed between neighbouring parallel or subparallel ridges. This is illustrated in figure 1. For a gully with steep walls, the wall on the same side as the Sun casts its shadow into the gully which then appears on the image as a line darker than its immediate neighbourhood. In the case of a valley formed between two ridges, the hillslope on the side opposite to the Sun receives a strong direct illumination while that on the same side as the Sun receives a weak indirect illumination since it is shaded. The strongly illuminated hillslope appears bright in the image while the other appears dark, thereby producing a sharp contrast. The valley is therefore represented by the edge between them. Although a crestline produces a similar effect on the image, since the position of the Sun is known, the following rule applies: when the shaded side is on the same side as the Sun with respect to the edge, the latter corresponds to a valley, whereas when it is on opposite sides with the Sun, the edge corresponds to a crestline. This contrasting property enables the discrimination between valleys and crestlines, thereby facilitating the detection of the former. In the case of occurrence of a lone ridge, although its crestline would still produce a sharp edge, there is no danger of such at the foot of the shaded side because, since there is no Sun-facing hillslope to create contrast on this side, shading smoothly diminishes downhill, and no edge is formed. Thus, the risk of lone ridges creating false channels in the image is low. In all cases, however, any of the above features whose azimuth is equal (or close) to the local azimuth of the Sun will be very weakly portrayed, if at all.

It is obvious that if certain other features (such as roads and other man-made features) present the same image facies as drainage channels, they would be detected in error. As algorithms are usually incapable of distinguishing desired features from artefacts, the easiest way to avoid interference from the latter is to use images where they are either non-existent or rare. Drainage channel detection from satellite images, as described in this paper, is therefore most applicable to undeveloped homogeneous terrains such as arid zones.

The steps involved in the multilevel extraction process presented in this work are the following. First, the image is preprocessed to enhance feature presentation. Then, edge detection is performed and the resulting edges are consolidated and skeletonized, reducing them to a network of one-pixel-wide line segments. This line image is the output of the lowest level of knowledge about channel network extrac-

tion, namely extracting candidate lines for networks. At the intermediate level of extraction, these line segments are sorted on the basis of knowledge about the local behaviour (Meisels 1991) of network elements. To achieve this, the line image is superimposed on the original image, and each segment is rated based on the shading conditions that apply along and around it. This process facilitates the differentiation between valleys and crestlines, and enables the estimation of the degree of qualification of each line segment as a possible channel element. Finally, at the highest level of knowledge, drainage channel networks are built up through a logical selection of highly rated segments and others satisfying certain conditions about network flow. This is clearly high level knowledge of flow channels that is domain dependent and is unrelated to generic image understanding techniques.

The entire channel network detection process presented in this work is fully automated. The intermediate and high level procedures are carried out by a single programme coded in C. We have tested our technique on a Landsat TM subscene of an area located in the Israeli Negev arid zone.

3. Low level image processing

The low level image processing involves image enhancement followed by edge extraction, consolidation, and skeletonization. The result is a network of lines to be used as input data for the higher level processes of this detection.

3.1. *Image enhancement*

The objective of image enhancement is to improve the portrayal of the desired feature in order to facilitate its extraction. Here, the feature of interest is the drainage channel. We tried several multi-band enhancement techniques including different image algebras between bands (such as ratios, vegetation indices, and so on), and spectral transformations such as the principal components and the intensity, hue and saturation analyses. But none of these gave a satisfactory result as far as our target feature is concerned. For example, ratio images tend to have much less contrast and more noise (Goetz 1989, p. 514); qualities that contradict the requirements for the current work. We, therefore, resorted to the use of a single band. We chose band 3 (red band) because it appears to be the one that offers the highest contrast in our image and expresses drainage features most clearly in our study area. The reason why this is so may be explained by the fact that solar radiation peak occurs in the visible portion of the electromagnetic spectrum and, within this visible portion, atmospheric scattering affects the red band much less than it does the other (blue and green) bands (see Mather 1987, chapter 1). However, our choice is based purely on visual comparison between the six reflective bands of our Landsat TM image. Thus, this choice is not strict; any other band could be used depending on circumstances. For instance, Wang *et al.* (1983) used the near-infrared band (0·8–1·1 μm) of Landsat MSS for a vegetated area because, among other reasons, green vegetation produces very high reflectance in this region and may not be mistaken for topographic shading. This consideration does not apply to our own case, since our study site is devoid of green vegetation. Figure 2 shows our test image which is composed of 500 × 500 pixels.

We tried several image enhancement operations on the single band and found out that, since the presence of drainage channels is mainly depicted by either dark lines on brighter backgrounds or edges between bright and shaded areas, it follows that the main, and virtually the only, preprocessing requirement in our case are

Figure 2. Input image (Landsat-TM band 3 of a part of the Israeli Negev arid zone, after linear stretching); 500 pixels by 500 pixels.

contrast and edge enhancements. As a first step towards achieving this, we performed contrast stretching. There are several methods of doing this of which the most standard are linear stretch, histogram equalization, and Gaussian stretch. We adopted linear contrast stretching because it is the only one that stretches the existing spectrum of grey levels linearly without redistribution of values; a process which may distort the hierarchical order of grey levels which forms the basis of our work.

After the contrast stretching, we applied an edge enhancement convolution filter using a 3 × 3 window. The following kernel was used:

$$
\begin{matrix}
0 & -1 & 0 \\
-1 & 5 & -1 \\
0 & -1 & 0
\end{matrix}
$$

As explained by Mather (1987), the application of this high-pass filter amounts to subtracting the Laplacian of an image from the image itself. This is equivalent to removing the diffused element of the signal from a given pixel (Mather 1987, p. 258).

3.2. *Edge detection and consolidation*

The detection of coherent edges suitable for use as a main structural framework for feature recognition and extraction has proven to be a goal-directed task. Several approaches have been proposed in the literature. Some of the most frequently cited examples include the works of Marr and Hildreth (1980), Haralick (1984), and Canny (1986). Since different edge extractors produce different results, there has been a great deal of argument in computer vision circles as to which approach is the optimal (Chen and Medioni 1989) but, it appears that performance is application

dependent. In other words, edges cannot be considered in isolation of the context of work. We tested several edge extractors (including those mentioned above) and each result was visually assessed with a view to selecting the one that best suits our purpose. We finally chose the Difference Recursive Filter (DRF) edge detector proposed by Shen and Castan (1986) because it gave the best performance for drainage channel detection, especially with regard to edge localization. The DRF edge detector is based on the difference between the input image and the output of a recursive symmetric exponential filter. Details of the mathematical basis of this edge detector are given in Shen and Castan (1986) and will not be discussed here. We used the DRF edge detector as it exists in the KHOROS Open Software Package available in many image processing laboratories. The user is required to supply numerical values for a number of parameters for which default values are also provided. After testing with different values, we found that the default values gave us the best result and we used them as such. The result of edge detection by the DRF is a binary edge image in which all edge pixels have the same value, 255, and other pixels form the image background with value 0. Our edge image is shown in figure 3.

In general, edge detection algorithms, including the DRF used in this work, usually do not recognize lines as single edges because they search mainly for abrupt changes in grey levels. Thus, if there is a line in the image, an edge is detected on both sides of it, even if it is only one pixel wide. In our case, a drainage channel (such as a gully) occurring as a line in the original image would yield two, close, quasi-parallel edges that touch intermittently. Neither of the two edges could be said to represent the original line. In order to recover the latter, first, a single edge is created from this dual edge by filling the space between them. We refer to this process
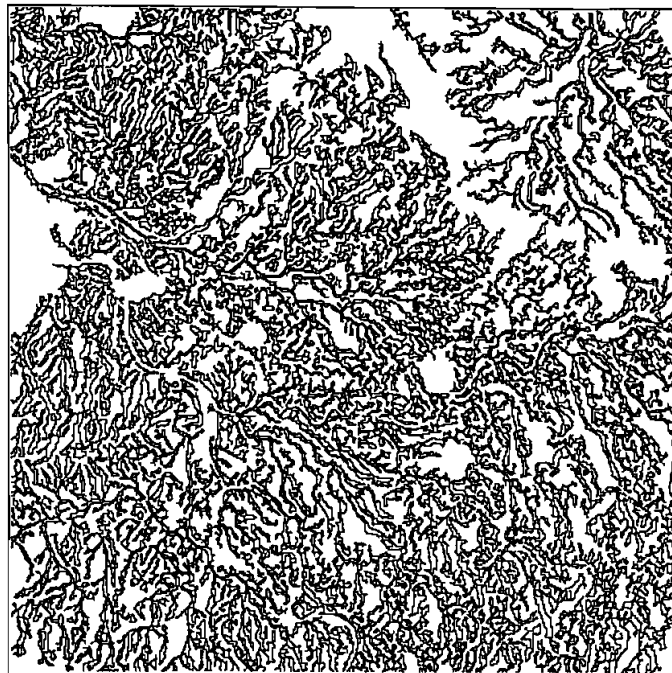

Figure 3.   Result of edge enhancement and edge detection performed on figure 2.

as 'edge consolidation'. Then the consolidated edge is skeletonized and the resulting line corresponds to the line formed by the drainage channel in the original image. To achieve consolidation, one-pixel-wide lines constituted by background pixels bordered on both sides by edge pixels are traced and their pixel values changed from 0 to 255.

3.3. Skeletonization

After the steps of edge detection and consolidation, the next step of low level processing is skeletonization in order to recover one-pixel-wide streamlined edges. For this purpose, we employed the parametrizable skeletonization algorithm proposed by Riazanoff *et al.* (1990). The details of the skeletonization algorithm are given in that paper and will not be reproduced here. The actual implementation employs an iterative procedure to remove object pixels (in this case, edge pixels) and replace them with background pixels based on the relative number and arrangement of object and background pixels in a 3×3 neighbourhood. We worked in the 8-connected mode in which all eight immediate neighbours of a central pixel are considered as its neighbours, as opposed to the 4-connected mode in which only those related to it in the horizontal or vertical sense are considered so. In Riazanoff *et al.* (1990), a contour pixel is defined as an object pixel with at least one background neighbour, while a connection pixel is defined as an object pixel linking at least two object parts. During iteration, only contour pixels may be removed. An important condition for the removal of a contour pixel is that its convexity K should be less than a threshold convexity K_T supplied by the user. The convexity K of a contour pixel is defined as the highest number of background pixels that are contiguous among its eight immediate neighbours. If, in the 3×3 neighbourhood, we denote the contour pixel by C, other object pixels by 1, and background pixels by 0, the following are examples of configurations for $K = 3$ to $K = 7$:

$$
\begin{array}{ccc}
1 \quad 0 \quad 0 \\
1 \quad C \quad 0 \\
0 \quad 1 \quad 1 \\
K = 3
\end{array}
\qquad
\begin{array}{ccc}
0 \quad 1 \quad 0 \\
0 \quad C \quad 1 \\
0 \quad 0 \quad 1 \\
K = 4
\end{array}
\qquad
\begin{array}{ccc}
1 \quad 0 \quad 0 \\
0 \quad C \quad 0 \\
1 \quad 0 \quad 0 \\
K = 5
\end{array}
\qquad
\begin{array}{ccc}
0 \quad 1 \quad 1 \\
0 \quad C \quad 0 \\
0 \quad 0 \quad 0 \\
K = 6
\end{array}
\qquad
\begin{array}{ccc}
1 \quad 0 \quad 0 \\
0 \quad C \quad 0 \\
0 \quad 0 \quad 0 \\
K = 7
\end{array}
$$

We carried out test skeletonizations with all possible convexity threshold K_T values (1 to 8) and found that 5 gave the best result; therefore, we used $K_T = 5$ in our work. In the process of skeletonization, for each iteration, the algorithm scans the image row after row. If a contour pixel is encountered, it can be removed only if: (1) its convexity K is less than the threshold convexity K_T; (2) it was not a connection point before the preceding iteration; and (3) it is not currently a connection point. The skeletonization process stops only after an iteration in which no pixel is removed in the entire image. The result obtained from skeletonizing our edge image is shown in figure 4. In this image, sets of one-pixel-wide line segments join in a seemingly haphazard manner, forming a complex line network of which the drainage channel network is a subset. The procedure for recovering channel networks from the skeletonized edge image employs higher levels of knowledge: intermediate level knowledge of shading conditions and local channel topography and high level knowledge of flow in channel networks. We turn next to the intermediate level processing and describe the grading of channel segments.
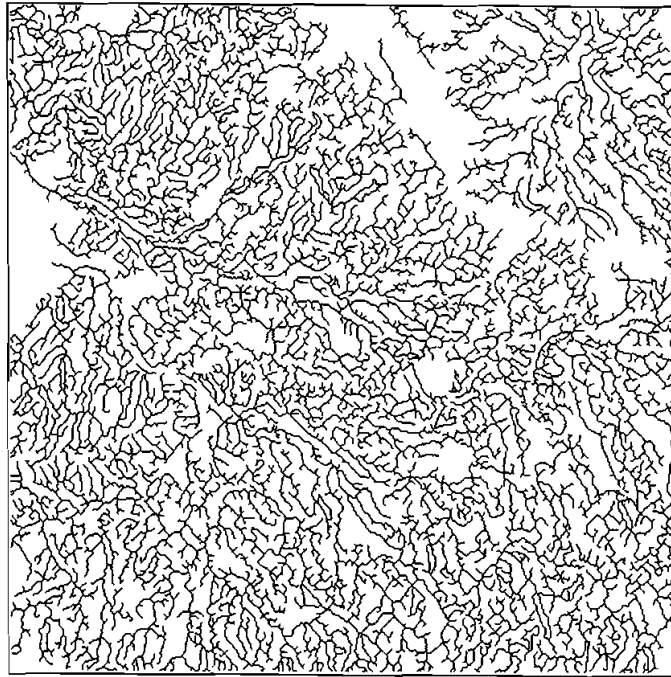
Figure 4.   Result of edge consolidation and skeletonization performed on figure 3.

4.   Intermediate level of extraction: rating from shading

The skeletonized edge image (figure 4) is composed of lines representing drainage channels as well as crestlines and other curvilinear features. In this intermediate level, these lines are rated (or graded), thereby quantifying them in readiness for the high level process of drainage channel detection. The basic element for this procedure is the unbranched line segment joining either two consecutive junctions or an extremity and the closest junction.

Each network of connected line segments is traced. Although tracing is done segment after segment, it is necessary that all interconnected line segments be traced as a set in order to establish the directional relation between them. This coordination will be of special usefulness during channel network reconstitution. Ichoku and Chorowicz (1994) recommend that the tracing of a channel network begin at the outlet and advance toward the various sources. This procedure cannot be strictly implemented in the current work because the input line networks are not pure channel networks since they are not only composed of channel elements but also of crestlines and other curvilinear features; all interconnected. As such, they do not have outlets. Therefore, the tracing of each of these line networks begins from the first encountered free end of a line. Each segment is traced by recursive displacement from pixel to pixel. When a junction is reached, the current segment is regarded as ended, and each branch is traced in turn in a similar fashion. This process continues until the whole line network is traced. During this process, each segment is assigned an identification number and its details are recorded in an array. These details include the coordinates of its beginning and end, the number of pixels of which it is composed, its direction, and the identification numbers of the segment before it and those succeeding it, including indications about how they are connected.

The major part of intermediate level processing is to apply knowledge about shading differences between gullies, valleys, and crestlines (with a given Sun azimuth) in grading segments. We have used a system of grading or rating which expresses a measure of the likelihood of a line segment to represent a drainage channel. The grades range from 0 (totally unlikely) to 10 (very likely). The grade or rating attributed to each segment is dependent upon the conditions of shading that gave rise to its formation in the image. Shading condition is estimated from the original stretched image (figure 2). To achieve this, each segment is superimposed on the image and the values of all image pixels underlying it are obtained and their mean computed. Also, image pixels bordering the segment on the left and right sides are obtained and a mean value is computed for either side. These mean pixel values on the segment and on its left and right sides are denoted by P_s, P_l, and P_r respectively. The computed values represent the average brightness expressed by the feature corresponding to the segment and by its immediate left and right borders respectively. In the rest of this discussion, for each segment, the smallest of the three values P_s, P_l, and P_r will be denoted by P_{min} and the largest by P_{max}.

The direction of a segment is measured as a whole-circle clockwise bearing (ranging from 0 to 360 degrees) referred to an axis parallel to the columns of the image. Since the segments are usually curved, in order to avoid bias, a least squares line is fitted to each segment, and the direction of this line becomes that of the segment. However, if the segment is composed of less than five pixels, its direction is computed from the coordinates of its two end points. The bearing of each segment from the Sun, denoted by B_{ss}, is computed from the direction of the segment and the azimuth of the Sun. This bearing shows the location of the Sun with respect to the segment. When the value of B_{ss} is between 0° and 180° the Sun is on the left of the segment, whereas when it is greater than 180° it is on its right. However, since no shading will be produced when the Sun is lying more or less in the direction of the segment, when the bearing is in the range $B_{ss} = 0° \pm 5°$ or $B_{ss} = 180° \pm 5°$ the Sun is considered not to be on the left or right of the segment. Thus, if we use PSUN to designate the position of the Sun relative to the segment then:

when

$$B_{ss} = 0° \pm 5° \text{ or } B_{ss} = 180° \pm 5°, \quad PSUN = C \text{ (centre)}$$

when

$$5° \leqslant B_{ss} \leqslant 175°, \qquad\qquad PSUN = L \text{ (left)}$$

when

$$185° \leqslant B_{ss} \leqslant 355°, \qquad\qquad PSUN = R \text{ (right)}$$

The rating of segments is achieved in two steps. First, the segments are classified into any one of the groups gully, valley, or crestline, then, segments belonging to each group are rated. The following gives the criteria for classifying a segment into any one of the groups:

(a) **Gully:**
$P_{min} = P_s$ and $PSUN = L$ or R

This is because, as demonstrated in figure 1, the average brightness of a gully

should be less than those of its two sides, when the Sun is not in the direction of the gully.

(b) **Valley:**

either $(P_{max} \neq P_s$ and $P_{min} = P_l$ and $PSUN = L)$

or $(P_{max} \neq P_s$ and $P_{min} = P_r$ and $PSUN = R)$

This is because the hillslope on the same side as the Sun (with reference to the edge) is shaded and should have the minimum average brightness, provided the average brightness of the segment itself is not the maximum.

(c) **Crestline:**

either $(P_{max} \neq P_s$ and $P_{min} = P_l$ and $PSUN = R)$

or $(P_{max} \neq P_s$ and $P_{min} = P_r$ and $PSUN = L)$

This is because the hillslope on opposite sides with the Sun (with reference to the edge) is shaded and should have the minimum average brightness, provided the average brightness of the segment itself is not the maximum.

(d) **Other:** Segments which cannot be classified into any of the above three classes are classified as **Other**. These include the following cases:

(i) Segments composed of just a single pixel which could not be classified because their parameters are indeterminable since they have no direction.

(ii) When $P_{max} = P_s$

This is a segment showing a higher average brightness than both of its sides. (It could be any highly reflecting curvilinear feature.)

(iii) When $PSUN = C$

This is a segment oriented in the direction of the Sun. (It may be any curvilinear feature with its own radiometric identity not related to shading.)

Segments belonging to the three known classes (Gully, Valley, and Crestline) are rated separately but in a uniform fashion. In each case, the rating value assigned to a segment depends on the value of P_{min}. The ratings applied are shown in table 1. In respect of the segments classified as Other, those composed of a single pixel are assigned the median rating value of 5 (because they have equal chances of being or not being channel elements) while the rest are assigned the value of 4 (because they

Table 1.   Categorization and rating of line segments based on shading conditions.

Range of the minimum mean pixel value	Ratings		
	Gully	Valley	Crestline
$0 \leqslant P_{min} \leqslant 25$	10	10	0
$25 < P_{min} \leqslant 50$	9	9	1
$50 \leqslant P_{min} \leqslant 75$	8	8	2
$75 \leqslant P_{min} \leqslant 100$	7	7	3
$100 < P_{min} \leqslant 125$	6	6	4
$125 < P_{min} \leqslant 150$	5	5	5
$P_{min} > 150$	4	4	4

have lesser chances of being channel elements, though there is still the possibility that they might be).

It is interesting to observe that the average pixel value for a shaded area is independent of the regional brightness of the zone where it is located. This is why the P_{min} values are used independently in the foregoing rating procedure. However, as these values are computed from the linearly stretched image, they can be regarded as standardized values because conventionally, images with full linear stretching have pixel values in the range of 0 to 255.

5. High level extraction: channel network construction

The high level part of network detection involves a logical build-up from a selection of the rated segments. Although a segment's rating indicates its likelihood as a drainage channel element, it is not a sufficient criterion for selecting a segment. This is because, due to some imperfections either in the imaging or one or more of the lower level processes, certain segments which actually represent channels might have low ratings whereas some others corresponding to other features might have high ratings. Therefore, in order to augment the robustness of the detection, knowledge of the principles of network formation and the topological relationships between network elements has been integrated in this process of network reconstitution.

It is assumed that drainage channel networks start as short segments which subsequently extend both upstream and downstream, each eventually joining a mainstream as a tributary and may itself constitute a mainstream to which other tributaries may join. Our high level extraction technique simulates this hypothesis. It starts from segments with very high ratings (8 to 10). Each of these starting segments is extended in both directions by progressively linking contiguous segments with ratings of 5 or higher which satisfy a certain condition of collinearity. Testing for linking involves the computation of the directional deflection or deviation between the last linked segment and each segment connected to it at the other end, whose rating is up to the threshold value (which is 5). Deflections to the left side are assigned a negative sign while those to the right are assigned a positive sign. Thus, the absolute deflection between any two directions can only be in the range of 0 to 180 degrees. The segment which offers the lesser absolute directional deflection is further tested for collinearity before it is linked. The condition adopted for collinearity is that the absolute value of the individual deflection should not exceed 30 degrees (60 degrees is allowed for segments shorter than five pixels, since such small segments are apt to produce wider deflections even when they are subsumed in a generally collinear series of segments) and the cumulative deflection over the linked series of segments should not exceed 90 degrees. Each linked series of segments (which we shall refer to as a 'series') is stored in an array together with its parameters. These include the identification numbers of its component segments, the total number of pixels, and its general direction. It is pertinent to mention that during the linking process series are not allowed to cross each other.

The heart of the high level construction process consists of channelling the series based on their topological interrelationship with one another. Channelling involves the determination of the sense of flow in each series based on its directional relation with other series connected to it. In what follows, we shall use the terms 'rear' and 'front' to refer respectively to the beginning and end of a series (or a single segment). These terms depict the sense in which the general direction of the series (or segment) is reckoned (i.e., from rear to front). A new orientation parameter has been introduced

to relate the actual sense of flow to the orientation of a series (or segment). This parameter has value 1 if it is determined that flow goes from front to rear, -1 if it goes from rear to front, and 0 if the sense of flow is not yet determined. In determining flow orientation on the basis of the directional relations between contiguous series, the basic assumption used is that a tributary joins a mainstream in such a way that flow does not deflect by more than 90 degrees. In our implementation, all possible configurations between contiguous series are taken into consideration. The acceptance of a series depends on its compatibility with its already accepted neighbours. In order that the acceptance of very short series which happen to have been encountered first does not ruin the chances of those of considerable length which may be encountered later, the series are processed from the longest to the shortest. Any series currently being considered may be referred to as the 'candidate series'. The following procedure has been used in processing each candidate series. It is evident that the algorithm will not be sufficiently clear to the reader if presented as a flowchart, so we have decided to give it in detail for clarity.

5.1. *Algorithm for the assessment of candidate series*

(*A*) If any of the series connected to the front end of the candidate series has been previously accepted (that series is denoted by front connection), perform the following:

- (*i*) Compute the directional deviation between the candidate series and the front connection.
- (*ii*) Determine whether the point of contact is at the front or rear end or somewhere in the middle of the front connection.
- (*iii*) If neither the candidate series nor the front connection is channelled, try to channel one or both of them using their directional deviation.
- (*iv*) If one of them is channelled, try to use it to channel the other one.
- (*v*) If both are channelled, determine whether they are compatible; without which the candidate series is rejected.

Figure 5 presents all the possible relations that may exist between a candidate series and a front connection. It illustrates the interplay of series orientation, directional deflection, and channelling orientation in determining whether or not a candidate series should be rejected.

(*B*) If the candidate series is not yet rejected, **then** if any of the series connected to the rear end of the candidate series has been previously accepted, denote it by rear connection and carry out a similar procedure to the one described above for front connection.

(*C*) If the candidate series is not yet rejected, **then** identify all its tributaries (i.e., all series and single segments that meet the threshold rating which are connected to the main body of the candidate series as opposed to its front or rear end) whether they have been accepted or not.

- (*i*) For all tributaries which correspond to already accepted series perform the following operations:
  - (*a*) Compute the directional deviation between the candidate series and each of the tributaries
  - (*b*) If the candidate series is not yet channelled, use the first of these tributaries to channel it

	Directional Dev. <= 90			Directional Dev. > 90		
Prior channelling orientations / Point of contact on front connec.	Rear end	Middle	Front end	Rear end	Middle	Front end
Front Connec. 0 / Candidate Ser. 0						
Front Connec. 0 / Candidate Ser. +1		R	R	R	R	
Front Connec. 0 / Candidate Ser. -1						
Front Connec. +1 / Candidate Ser. 0		R	R			
Front Connec. +1 / Candidate Ser. +1		R	R	R	R	R
Front Connec. +1 / Candidate Ser. -1	R	R	R			
Front Connec. -1 / Candidate Ser. 0				R	R	
Front Connec. -1 / Candidate Ser. +1	R	R	R	R	R	
Front Connec. -1 / Candidate Ser. -1				R	R	R

LEGEND

/ Front Connection	/ Candidate Series	R Case of Rejection of Candidate Series

Figure 5. Sketches of possible topological relations that may exist between a candidate series and a front connection. Arrows indicate the sense of direction reckoning. A branch is attached to each already channelled series (either candidate series or front connection or both) in order to better depict the general configuration. Boxes marked with R at the lower right-hand corner represent configurations in which the candidate series is rejected.

(c) Once the channelling of the candidate series is established, if any of these accepted tributaries would join it in a contradictory sense, reject the candidate series

(d) Channel any of these accepted tributaries yet unchannelled

(ii) If the candidate series is not yet rejected **and** is not yet channelled, it follows that none of its tributaries has been accepted. **Then** for all the tributaries (using only the segments directly connected to the candidate series) perform the following:

(a) Compute the directional deviation of each of them from the candidate series

(*b*) Distinguish those making directional deviations of 90 degrees and under from those making more than 90 degrees (segments belonging to each group are not simply counted, rather, their rating values are summed up, in order that rating may be given due consideration)

(*c*) Channel the candidate series based on the group with the higher sum of ratings

(*D*) If the candidate series is not yet rejected, **then** if it is channelled but any of its connections (front or rear) is not channelled, **then** repeat all of the above steps in order to channel all the connections.

(*E*) If the candidate series is not yet rejected, **then** for each of its connections (including tributaries) which has been channelled in the current process, propagate channelling from connections to connections-of-connections, until all previously accepted series which are directly or remotely connected to the current series are channelled. If any channelling contradiction is detected (even at this stage), **then** reject the candidate series.

(*F*) If the candidate series is not yet rejected, **then**

(*i*) Accept it.

(*ii*) If it is channelled, **then** accept its single segment tributaries which conform with its channelling (do not accept tributaries which are series; series can only be accepted when they are processed as candidate series).

After processing all the series currently acquired, the detected channels (comprising all series and single segments accepted in the foregoing algorithm) would constitute only portions of networks separated from one another. To improve the connectivity between them, more series must be processed. Unlike the first set of series, subsequent sets are not obtained from independent locations but at extensions of already detected portions of networks. In the second phase, series may be taken from the extensions of different parts of the existing portions of networks to enable further extension of channels in accordance with the principle of channel network formation described above. This process will also provide an opportunity to determine the channelling of some of the unbranched portions which are yet unchannelled. This second set of series is acquired with a lower rating threshold (we set the threshold value to 4). They are processed exactly the same way as the previous ones except that priority is not given to length of series any more. Series are treated on the basis of first-acquired-first-processed. Even though the rating threshold is lowered, if any of the series meets the set topological criteria, it is integrated as part of the network whose extension it is. This is because, as previously stated, certain legitimate parts of the network may have low rating values due to a variety of factors. After the second phase, the main structure of the network is established, although there would still be gaps. In order to try to fill up gaps, to obtain more connectivity in the channel networks presently detected as well as more continuity in flow, a third phase of acquiring and processing of series is embarked upon. In this phase, the series are taken only at extensions of the actual downstream end of each of the currently existing portions of networks. The rating threshold value of 1 is used this time. The threshold has been brought so low to prevent rating values from singly constituting an impediment to the continuity of flow. The idea is to route flow as much as possible. However, each series is subjected to the same topological tests described in the algorithm above, and is accepted only if it passes them. This third
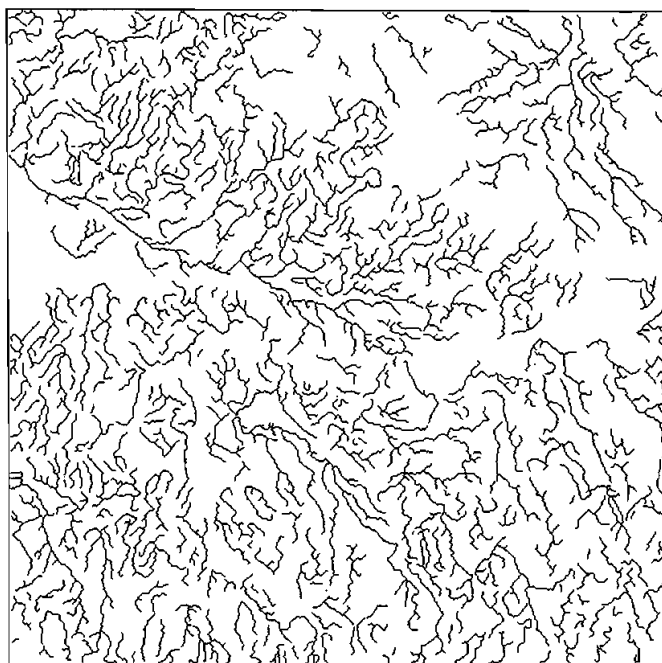
Figure 6. The final result of the computerized drainage channel network detection.

phase is performed iteratively until no more series qualifies in the entire image. Throughout the entire operation, the rating threshold value for considering single segments as tributaries remains 5, because such single segments usually do not have continuity at the other end, and when they have low ratings, they are probably not channels. The final result of this high level stage of the processing is shown in figure 6.

6. Evaluation of the extraction process and result

Images portraying natural scenes normally contain a wide variety of features as well as noise. Computerized detection of one or more specific features from such images is not an easy task. There are numerous practical difficulties that hamper the smooth implementation of feature detection. First, it is not all image characteristics of a feature that can be integrated in algorithms. Even those that can be integrated are not exclusive to one or a clearly distinct group of features. Secondly, noise and other factors may, on one hand, suppress certain characteristics of the target features thereby hindering their detection, and on the other hand, modify those of other features causing them to respond to detection erroneously. In our specific case of drainage channel network detection from digital satellite images, we have been faced with several difficulties. The current discussion tries to highlight some of the practical problems associated with this work. We expect that they will be of some relevance to future investigations in this domain.

Drainage features are three-dimensional but are imaged in two dimensions. This dimensionality degradation is not peculiar to drainage features, as all images represent objects in two dimensions even though most objects are three-dimensional in reality. To facilitate detection, such objects may either produce a well-defined spectral thumbprint or signature, or have a recognizable geometric shape, relative size or

location. Drainage features lack all of these except in special cases when they bear water (which has a spectral signature). In general, all that is known is that they are curvilinear features which appear as edges or lines in images and which are sometimes connected. It is obvious that these characteristics may also apply to other features, of which typical examples include crestlines, roads and other tracks, and even lithological boundaries and other natural and artificial boundaries. In our intermediate level processing of the skeleton image of edgelets (figure 3) we use domain specific knowledge of shading conditions to enable a rough differentiation between crestlines and drainage channels. However, we find that this level of processing and the level of knowledge which it uses (Meisels 1991) is still insufficient. As a result, we apply higher level knowledge about the order of precedence in channel network formation as well as the topological relations between network components. Even then, channels with the same azimuth as the Sun may not be clearly expressed in the image and very wide channels are difficult to detect because in the automatic mode there is no way of distinguishing their image presentation from that of other areas.

Some of the errors that may have occurred in this work may be attributed to the low level processes. Although the purpose of these processes is to provide a suitable background for enhanced higher level detection, sometimes due to certain imperfections, they may yield poor results. In edge detection for instance, accurate localization of detected edges is of crucial importance, yet it is one of the most difficult aspects in this type of work. It is obvious that once an edge is wrongly localized, all subsequent values computed for use in its evaluation as a drainage channel will be wrong. Furthermore, at the occurrence of a line, like any other edge detector, ours detects a dual edge. In order to recover the original line, this dual edge is consolidated, then subjected to skeletonization. If the resulting line is wholly or partially shifted with respect to the line it represents in the original image, then some or all pixels used for the computation of rating (at the intermediate level) are taken from wrong locations, resulting in an erroneous rating value. However, in this work, we have tried to use one of the best currently available edge detectors as far as the quality of localization is concerned, thus curbing the error sources.

The high level channel detection process may also have been affected by a number of problems. The topological concept which has been applied in this detection is based on the assumption that the deflection made by flow in moving into a stream from its tributary does not exceed 90 degrees. Although this is the general rule for the common types of channel patterns such as dendritic and parallel, it is not always true for other types such as some trellis and rectangular networks (Ichoku and Chorowicz 1994) and for some cases of drainage anomalies (Howard 1967). Non-conformity with directional deflection specifications may have resulted in the disqualification of a number of candidate series which would have qualified otherwise. It has not been possible to avoid this in our investigation, because there is no way of identifying such segments in order to accord them special considerations. One other source of inconvenience in the detection process relates to the fact that the qualification of a series (or a single segment) depends on its relationship with other already qualified ones with which it has connection. Thus, any non-channel feature which happens to have qualified erroneously may prevent the qualification of a legitimate piece of channel that is tested by the extraction procedure after it has accepted the erroneous feature. In any case, the approach used is justified because series must be processed one after the other and consideration must be given to topological interrelationships.
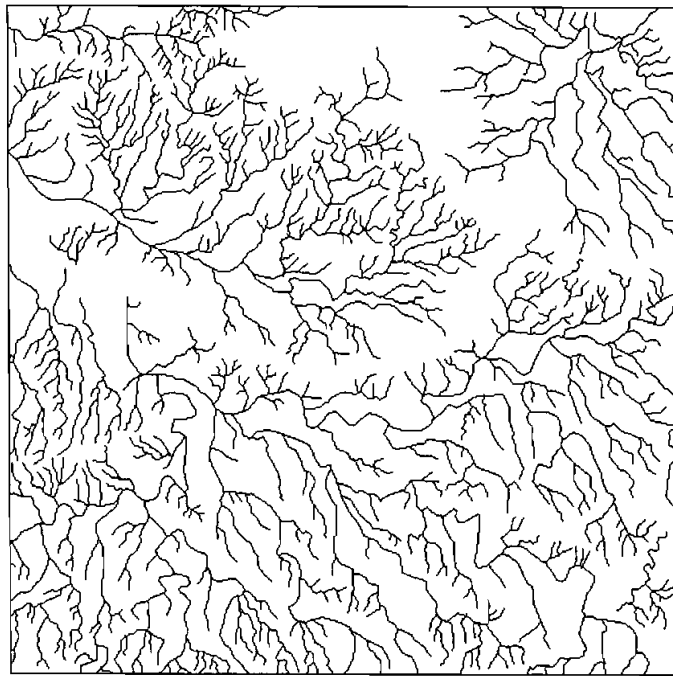
Figure 7. Channel networks manually extracted from the original image shown in figure 2.

To do some appraisal of our final result (figure 6), we carried out a manual extraction of channel networks from a hardcopy of the original image (figure 2). Figure 7 shows the result of manual extraction. A visual comparison of figures 6 and 7 shows that there is a substantial agreement between them; a proof of the high capacity of our computerized approach to detect drainage features from satellite images.

However, in order to be able to relate our results to a standard that would be as close as possible to the truth, we performed a manual extraction of channel networks from a topographical map of scale 1:50000. The map-extracted network is shown in figure 8. Since our image was not geometrically corrected, there is some geometric distortion in figures 6 and 7 (image products) with respect to figure 8 (map product), and their boundaries do not match exactly. For this reason and due to the slight shifts that may have affected the extracted channels, it is not possible to compare the extracted networks quantitatively; although the correspondence between them is quite evident visually. We can, however, make a qualitative comparison between these networks, bearing in mind that the map network (figure 8) is assumed to be the closest to the truth. We have chosen to measure their various qualities on a scale of: *poor, fair, very fair, medium, high, very high, excellent*. Table 2 shows our assessment of the network qualities. The criteria considered are the following:

1. **Coverage:** This represents the extent to which the extracted networks cover all parts of the data source (image or map) where channels exist.

2. **Connectivity:** This indicates the extent of connection between extracted channels relative to their connection in reality.

3. **Purity:** This expresses the relative amount of extracted channels that actually represent real channels (and not other features or artefacts).
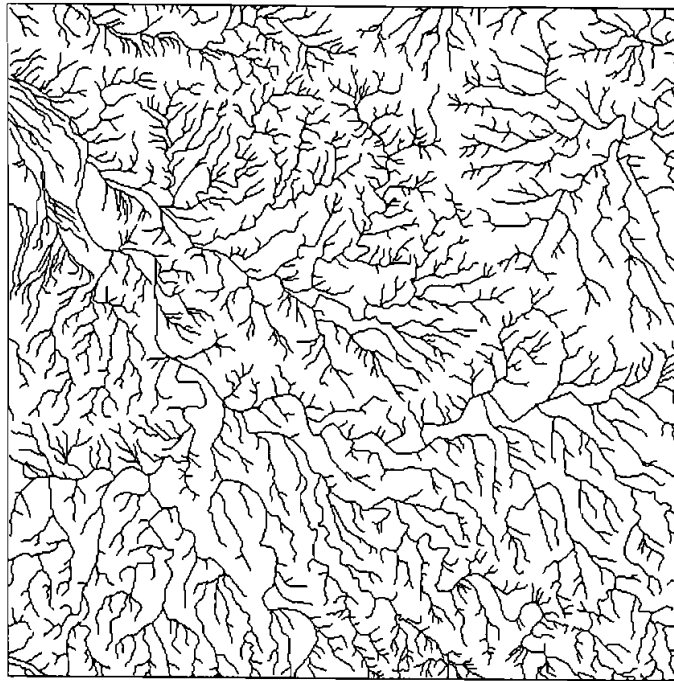
Figure 8. Channel networks manually extracted from a 1:50000 scale topographic map.

4. **Accuracy of localization:** This is a measure of the location of extracted channels relative to their location in the data source.

Based on the foregoing criteria and on our assessment as given in table 2, the manual extraction performs a little better than our computerized detection method only in terms of connectivity and purity. These few gaps and artefacts occurring in the result of the computer detection (figure 6) are probably due to the effect of some of the factors discussed in the first four paragraphs of this section. On the other hand, manual extraction processes enjoy much higher level of knowledge than can be incorporated in a computer programme. For instance, the human extractor has a global view of the image and can easily know the general character of the network. Also, he usually exercises much freedom in dealing with exceptional cases.

Table 2. Qualitative comparison between channel networks extracted from a topographic map and those extracted from the image manually and automatically. The scale of comparison is constituted by: poor, fair, very fair, medium, high, very high, excellent.

Network quality	Map network	Assessment	
		Manually extracted network	Automatically detected network
Coverage	Excellent	Very high	Very high
Connectivity	Excellent	Very high	High
Purity	Excellent	Very high	High
Accuracy of localisation	Very high	Very high	Very high

Nevertheless, the computerized detection process presented here has been very successful. Moreover, considered in the context of such inherent advantages of computerized approaches as rapidity and consistency, it can be said that this technique shows great potential.

7. Conclusion

This paper has demonstrated the capability for detecting drainage channel networks from digital satellite images (especially of arid regions). The methodology developed here covers a wide spectrum of image processing and pattern recognition techniques which fit the structure of multi-level architectures for Image Understanding (Meisels 1991). The detection of drainage channel networks on satellite images is a complicated task because channel networks do not have substantial image attributes that would facilitate their detection. They do not fall within any specific range in the greyscale, neither do they have a spectral signature. Furthermore, neither channel networks nor their parts exhibit any defined shape, size, orientation, or other unique quantitative characteristics, either relatively or absolutely. This may be why the prospect of performing this detection has hitherto not offered any significant appeal to researchers.

Despite the inherent handicaps and the generalizations applied to cope with them in certain steps of the detection process, the result has been satisfactory. This successful achievement may be attributed to two main factors. The first one concerns the study area. It is an arid zone with extremely sparse low vegetation. Also, lithological differences are not prominent and other curvilinear features such as roads are rare. Furthermore, most of the channels appear prominently on the image, few have the same azimuth as the Sun, and there are very few wide channels. The second factor relates to the fact that good knowledge-based techniques, embodied in a multi-level approach, have been applied in the detection process. For instance, at the high level stage, the drainage channel network was reconstituted by applying knowledge about channel network formation procedures and the common topological dispositions. The visual comparison between the final result of this extraction process and that of the human expert is very encouraging. Although our technique has been tested on the image of an arid region, we believe that it can also be applied to areas with smooth uniform vegetation cover.

The methodology presented in this work has high potentials for even better performance if further improvement is achieved in the associated techniques such as image enhancement, image segmentation, filtering, and edge detection. Furthermore, as modern spatial data handling techniques tend towards the use of Geographical Information Systems (GIS), if our methodology is adapted and operated under this framework—whereby complementary information can be derived from other sources—its efficiency will be further enhanced, such that its application can even be extended to other (non-arid and heterogeneous) situations with improved results.

References

ASTARAS, T., 1985, Drainage network analysis of LANDSAT images of the Olympus-Pieria mountain area, northern Greece. *International Journal of Remote Sensing*, **6**, 673–686.
ASTARAS, T., LAMBRINOS, N., and SOULAKELLIS, N., 1990, A drainage system analysis evaluation of, and comparison between, Landsat-3 RBV, Landsat-5 TM and SPOT PA imageries covering the Central Macedonia district, Greece. *International Journal of Remote Sensing*, **11**, 1549–1559.

BENHAMOU, M., 1987, Déscription et simulation de réseaux de drainage par analyse d'images, Doctoral thesis, Ecole Nationale Supérieure des Mines, Paris, France.

CANNY, J., 1986, A computational approach to edge detection. *I.E.E.E. Transactions on Pattern Analysis and Machine Intelligence*, **8**, 679–698.

CHEN, J. S., and MEDIONI, G., 1989, Detection, localization, and estimation of edges. *I.E.E.E. Transactions on Pattern Analysis and Machine Intelligence*, **11**, 191–198.

CHOROWICZ, J., ICHOKU, C., RIAZANOFF, S., KIM, Y.-J., and CERVELLE, B., 1992, A combined algorithm for automated drainage network extraction. *Water Resources Research*, **28**, 1293–1302.

FREDEN, S. C., and GORDON, F., 1983, Landsat satellites. In *Manual of Remote Sensing*, 2nd edition, vol. 1, edited by D. S. Simonett and F. T. Ulaby (Falls Church, Virginia: American Society of Photogrammetry), pp. 517–570.

GOETZ, A. F. H., 1989, Spectral remote sensing in geology. In *Theory and Applications of Optical Remote Sensing*, edited by G. Asrar (New York: John Wiley and Sons), pp. 491–526.

HARALICK, R. M., 1984, Digital step edges from zero-crossings of second directional derivatives. *I.E.E.E. Transactions on Pattern Analysis and Machine Intelligence*, **6**, 58–68.

HOWARD, A. D., 1967, Drainage analysis in geologic interpretation: a summation. *American Association of Petroleum Geologists Bulletin*, **51**, 2246–2259.

ICHOKU, C., and CHOROWICZ, J., 1994, A numerical approach to the analysis and classification of channel network patterns. *Water Resources Research*, **30**, 161–174.

MARR, D., and HILDRETH, E., 1980, Theory of edge detection. *Proceedings of the Royal Society of London*, **B207**, 187–217.

MATHER, P. M., 1987, *Computer Processing of Remotely-Sensed Images: An introduction* (Chichester: Wiley & Sons).

MEISELS, A., 1991, Levels of knowledge for object extraction. *Machine Vision and Applications*, **4**, 183–192.

RIAZANOFF, S., CERVELLE, B., and CHOROWICZ, J., 1990, Parametrizable skeletonization of binary and multilevel images. *Pattern Recognition Letters*, **11**, 25–33.

SHEN, J., and CASTAN, S., 1986, An optimal linear operator for edge detection. *Proceedings of I.E.E.E. Computer Society Conference on Computer Vision and Pattern Recognition, Miami Beach, Florida, 22–26 June* (Washington: D.C.: I.E.E.E. Computer Society), pp. 109–114.

WANG, S., ELLIOTT, D. B., CAMPBELL, J. B., ERICH, R. W., and HARALICK, R. M., 1983, Spatial reasoning in remotely sensed data. *I.E.E.E. Transactions on Geoscience and Remote Sensing*, **GE-21**, 94–101.